

Cite this: *Dalton Trans.*, 2011, **40**, 11562

www.rsc.org/dalton

PAPER

Experimental and computational exploration of the dynamic behavior of (PNP)BF₂, a boron compound supported by an amido/bis(phosphine) pincer ligand†

Jessica C. DeMott,^a Panida Surawatanawong,^{‡a} Shoshanna M. Barnett,^b Chun-Hsing Chen,^b Bruce M. Foxman^b and Oleg V. Ozerov^{*a}

Received 21st June 2011, Accepted 11th August 2011

DOI: 10.1039/c1dt11172h

The diarylamido/bis(phosphine) PNP pincer ligand (2-*i*-Pr₂P-4-MeC₆H₃)₂N has been evaluated as a scaffold for supporting a BF₂ fragment. Compound (PNP)BF₂ (**6**) was prepared by simple metathesis of (PNP)Li (**5**) with Me₂SBF₃. NMR spectra of **6** in solution are of apparent C₂ symmetry, suggestive of a symmetric environment about boron. However, a combination of X-ray structural studies, low-temperature NMR investigations, and DFT calculations consistently establish that the ground state of this molecule contains a classical four-coordinate boron with a PNBf₂ coordination environment, with one phosphine donor in PNP remaining “free”. Fortuitous formation of a single crystal of (PNP)BF₂·HBF₄ (**7**), in which the “free” phosphine is protonated, furnished another structure containing the same PNBf₂ environment about boron for comparison and the two PNBf₂ environments in **6** and **7** are virtually identical. DFT studies on several other diarylamido/bis(phosphine) pincer (PNP)BF₂ systems were carried out and all displayed a similar four coordinate PNBf₂ environment in the ground state structures. The symmetric appearance of the room-temperature NMR spectra is explained by the rapid interconversion between two degenerate four-coordinate, C₁-symmetric ground-state forms. Lineshape analysis of the ¹H and ¹⁹F NMR spectra over a temperature range of 180–243 K yielded the activation parameters Δ*H*[‡] = 8.1(3) kcal mol⁻¹ and Δ*S*[‡] = -6.0(15) eu, which are broadly consistent with the calculated values. Calculations indicate that the exchange of phosphine donors at the boron center proceeds by an intrinsically dissociative mechanism.

Introduction

Diarylamido/bis(phosphine) anionic PNP pincer ligands have given rise to a variety of exciting chemistry developments for the transition metal series.^{1–4} There have been fewer applications of these ligands in supporting main group compounds. We reported five-coordinate (PNP)AlX₂ complexes (*e.g.*, **1**) in 2007,⁵ which may be described as 10-Al-5 according to Arduengo's N-X-L nomenclature (illustrated in Fig. 1)⁶ which is most useful for hypercoordinate^{7–15} compounds. Parkin *et al.* described closely

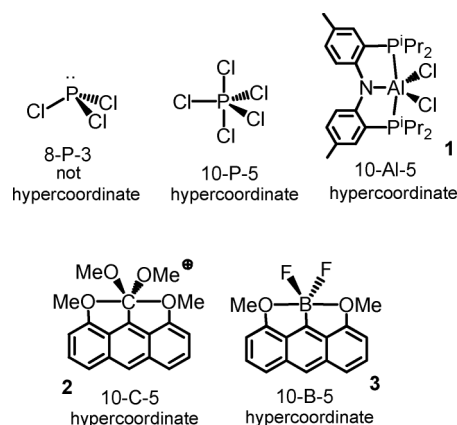


Fig. 1 Illustration of the Arduengo N-X-L nomenclature.

analogous 10-X-5 Ga and In PNP complexes in 2010.¹⁶ In collaboration with the Mindiola group we have also reported (PNP)TI.¹⁷ We were intrigued by the question of what coordination environments may be possible with a lighter, smaller¹⁸ main group element in the PNP system. Our interest was in part inspired by the successes of Akiba, Yamamoto and coworkers in isolating unusual

^aDepartment of Chemistry, Texas A&M University, College Station, TX, 77843-3255, USA. E-mail: ozerov@chem.tamu.edu

^bDepartment of Chemistry, Brandeis University, 415 South Street, Waltham, MA, 02454, USA

† Electronic supplementary information (ESI) available: Crystallographic information, coordinate tables for the calculated structures, selected pictorial NMR spectra and representations of calculated molecular orbitals. CCDC reference numbers 831094 and 831095. For ESI and crystallographic data in CIF or other electronic format see DOI: 10.1039/c1dt11172h

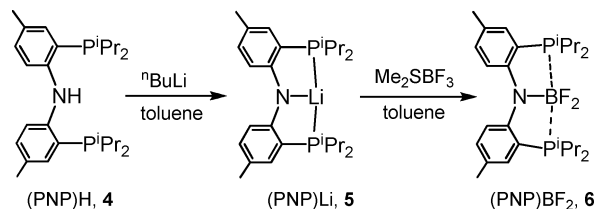
‡ Current address: Department of Chemistry, Faculty of Science, Mahidol University, 272 Rama VI Road, Phayathai Ratchathewee, Bangkok 10400, Thailand.

hypercoordinate compounds of carbon (**2**) and boron (**3**).^{19–26} These molecules followed a decades-long quest for stable ground state analogs of the transition state in the S_N2 reaction.²⁷ The designs of Akiba and Yamamoto (*e.g.*, **2** and **3**) benefit from a rigid framework encapsulating the focal carbon or boron atom. From an organometallic chemist's perspective, this framework can be viewed as a tridentate, anionic, meridional “OCO” pincer-style²⁸ “ligand” supporting a CX_2^+ or a BX_2 fragment. In the present work, we report our combined experimental and computational investigation of the dynamic nature of the compound in which a BF_2 fragment is supported by the PNP pincer ligand and the predicted influence of the possible ligand modifications. Ground-state pentacoordination at boron appears to be unavailable in these systems, and, surprisingly, even the transition-state 10-B-5 structures are not likely.

Results and Discussion

Synthesis of (PNP)BF₂ (**6**)

Reaction of (PNP)Li (**5**),²⁹ prepared *in situ* from (PNP)H (**4**)² and ⁿBuLi, with Me₂SBF₃ in aromatic solvents produced the desired (PNP)BF₂ (**6**) in 66% yield following workup and isolation (Scheme 1). This reaction is sensitive to light and should be performed in the dark. Utilization of Et₂OBF₃ instead of Me₂SBF₃ led to a greater amount of undesirable side products that proved difficult to separate. It is possible that the Et₂OBF₃ contained or accrued a greater amount of Brønsted acid impurity. The reactions worked best with freshly opened Me₂SBF₃.



Scheme 1 Preparation of (PNP)BF₂ (**6**) from (PNP)Li (**5**).

Compound **6** is a white solid that is soluble in aromatic solvents and CH₂Cl₂. It is stable in C₆D₆ solution when kept in the dark. Exposure to light, especially direct sunlight or artificial UV light led to decomposition. Compound **6** is visibly luminescent when subjected to sunlight near a laboratory window or artificial UV light.

NMR studies of (PNP)BF₂ (**6**) at RT

At ambient temperature, the ¹H NMR spectra of **6** display apparent C₂ symmetry. For example, the isopropyl groups give rise to four Me resonances (each a doublet of doublets, $J_{HH} = 7$ Hz, $J_{PH} = 14$ –15 Hz), and two multiplet CH resonances. (PNP)AlCl₂ (**1**) and (PNP)AlMe₂ display C₂ symmetry in solution, akin to **6**.⁵ In contrast, other square-planar d⁸ (PNP)MX complexes appear to be primarily C_{2v} symmetric, the highest possible for a PNP complex.³ We tentatively attributed the reduction in symmetry in **1** and (PNP)AlMe₂ to the restricted conformational movement of the P'Pr₂ groups that may cause the lowering of the time-averaged molecular symmetry even if the immediate environment about the central atom is C_{2v}-symmetric on the NMR timescale.

Table 1 Heteronuclear coupling constants (in Hz) determined by using the WinDNMR³⁰ to model the observed multiplets in the ¹¹B{¹H}, ¹⁹F, and ³¹P{¹H} spectra of (PNP)BF₂ (**6**)

Spectrum	J_{B-F}	J_{B-P}	J_{F-P}
¹¹ B{ ¹ H}	57 ± 2	69 ± 2	
¹⁹ F	55 ± 5		75 ± 5
³¹ P{ ¹ H}		68 ± 4	72 ± 4

We have also obtained ¹⁹F, ³¹P{¹H}, and ¹¹B{¹H} NMR spectra of **6** at ambient temperature. For each nucleus, one multiplet resonance was observed. In the first approximation, the multiplets reflected a P₂BF₂ system where the three requisite coupling constants are similar. Because of this, the ¹¹B{¹H} multiplet resembled a proper quintet (near-equal coupling to four $S = \frac{1}{2}$ nuclei), while the ¹⁹F and especially the ³¹P{¹H} multiplets resembled the 1:3:4:4:3:1 multiplets one would expect from near-equal coupling to two $S = \frac{1}{2}$ and one $S = \frac{3}{2}$ nucleus. More precise estimation of the coupling constants was accomplished by modeling the observed multiplets using WinDNMR³⁰ simulations (Table 1). Notably, the determined J values from different spectra agree well with each other. The differences in the coupling constants are obscured by the broadness of the lines in the multiplets, which is likely the influence of the quadrupolar ¹¹B nucleus.

All in all, the ambient temperature NMR analysis indicated a C₂ symmetric structure for **6**. In order to elucidate whether this was truly owing to a symmetric five-coordinate geometry at boron or merely to a time-averaged exchange of lower-symmetry classical structures, we carried out solid-state structural studies and low-temperature NMR experiments.

Solid state structures determined by X-ray diffraction

An X-ray structural study was conducted on a single crystal of **6** (Fig. 2). In the solid state, the molecule is decidedly dissymmetric with one of the phosphine arms of the PNP ligand turned away from and not bound to the boron center. The separation between the phosphorus atom in this phosphine arm and the boron atom is

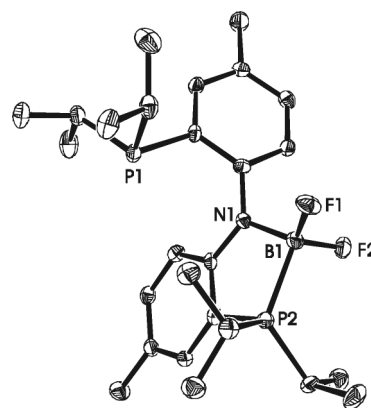


Fig. 2 ORTEP³¹ drawing (50% probability ellipsoids) of **6** showing selected atom labeling. Hydrogen atoms are omitted for clarity. Selected bond distances (Å) and angles (deg) follow: P2–B1, 2.046(4); F1–B1, 1.388(4); F2–B1, 1.394(4); N1–B1, 1.534(4); P2–B1–N1, 97.62(19); P2–B1–F2, 107.8(2); N1–B1–F2, 114.5(3); P2–B1–F1, 114.3(2); N1–B1–F1, 112.2(3); F2–B1–F1, 109.8(3).

well beyond bonding distance, and the lone pair of this phosphine is not directed at the boron atom. The other phosphine is bound to the boron atom, as is the N of PNP. The distorted tetrahedral coordination environment about the boron center is completed by two fluorides. The deviations from a perfect tetrahedron are likely caused by the angular constraint imposed by the P/N chelate and by the different nature of the four substituents.

While attempting to grow crystals of **6**, we inadvertently obtained a small quantity of single crystals of compound **7** (Fig. 3). X-ray structural data indicated that **7** is the BF_4 salt of a cation resulting from protonation of the “free” phosphine in **6**. HBF_4 was likely generated by adventitious hydrolysis of BF_3 *in situ* or is present as an impurity in the reagent itself. The structure of the cation of **7** is quite similar to that of **6** itself. The major difference is that the non-boron bound, protonated phosphine arm in **7** is closer to the PNBF_2 unit, ostensibly because of hydrogen bonding between H1 of the phosphonium and F2 of the PNBF_2 unit ($d(\text{H1}-\text{F2}) = 2.34(2)$ Å). However, there is remarkably little difference between the PNBF_2 units in **7** and **6**. The B1–F2 bond (F2 participates in hydrogen bonding) in **7** does not differ from the B1–F1 bond length or from the B–F bond lengths in **6**. The phosphonium hydrogen H1 also has relatively close contacts with the N of PNP ($d(\text{H1}-\text{N1}) = 2.62(2)$ Å) and one of the BF_4 anion fluorines ($d(\text{H1}-\text{F6}) = 2.62(2)$ Å). The B–F bond involving this fluorine in BF_4 is slightly longer than the average of the other three, but the difference is nearly statistically insignificant. In fact, the shortest and the longest of all 8 B–F bond lengths in **6** and **7** differ by only *ca.* 0.03 Å. B–F bond lengths of 1.38–1.40 Å are common for four-coordinate adducts of (amido) BF_2 compounds.³²

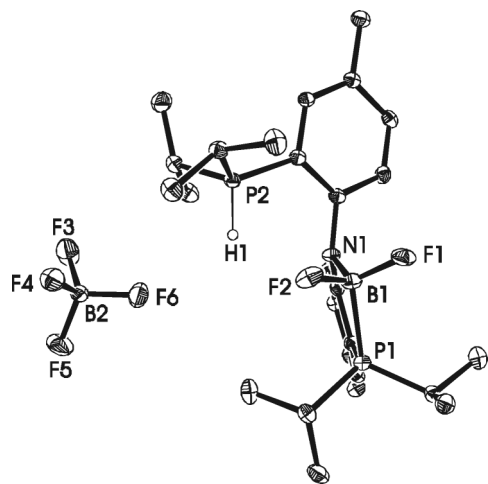


Fig. 3 ORTEP³¹ drawing (30% probability ellipsoids) of **7** showing selected atom labeling. Hydrogen atoms (except H1) are omitted for clarity. Selected bond distances (Å) and angles (deg) follow: B1–F1, 1.384(4); B1–F2, 1.396(4); B1–P1, 2.019(4); B1–N1, 1.550(4); P2–H1, 1.31(3); B2–F3, 1.382(4); B2–F4, 1.377(4); B2–F5, 1.365(4); B2–F6, 1.391(4); F1–B1–F2, 109.3(3); F1–B1–P1, 111.4(2); F2–B1–P1, 111.2(2); F1–B1–N1, 112.5(3); F2–B1–N1, 112.8(3); P1–B1–N1, 99.3(2).

The P–B bonds in **7** (2.019(4) Å) and **6** (2.046(4) Å) are similar to the crystallographically determined P–B bond length of 2.028(1)³³ Å in $\text{Et}_3\text{P}-\text{BF}_3$ and the calculated P–B bond length of 2.046³⁴ Å or 2.055³⁵ Å in $\text{Me}_3\text{P}-\text{BF}_3$. These distances are

also similar to the B–P distance in triorganophosphine adducts of $\text{B}(\text{C}_6\text{F}_5)_3$.³⁶

Low temperature NMR studies of (PNP) BF_2 (**6**)

A study of a CD_2Cl_2 solution of **6** by NMR spectroscopy in the +23 to -93 °C range revealed an eventual lowering of the symmetry from C_2 to C_1 , evident from the decoalescence of the corresponding ^{19}F , ^{31}P , and ^1H resonances at -61 °C or below (Fig. 4–7). The NMR spectra of **6** at -93 °C are consistent with the solid-state structure determined by X-ray diffraction (*vide supra*). The two fluorine nuclei resonated at two different frequencies (δ -138 and -145 ppm) as broad peaks (consistent with coupling to ^{11}B , ^{31}P and presumably each other). The $^{31}\text{P}\{^1\text{H}\}$ resonances decoalesced only at -83 °C or below, probably because of the small difference between the chemical shifts of the two exchange sites. Most tellingly, one of the $^{31}\text{P}\{^1\text{H}\}$ resonances at -93 °C is broad (from coupling to two ^{19}F nuclei and one ^{11}B), while the other one is relatively sharp (presumably, the “free” phosphine). The ^1H NMR spectra at low temperatures are likewise indicative of C_1 symmetry. The ^{11}B NMR signal broadens upon cooling to -80 °C, but remains a single resonance (Fig. 8).

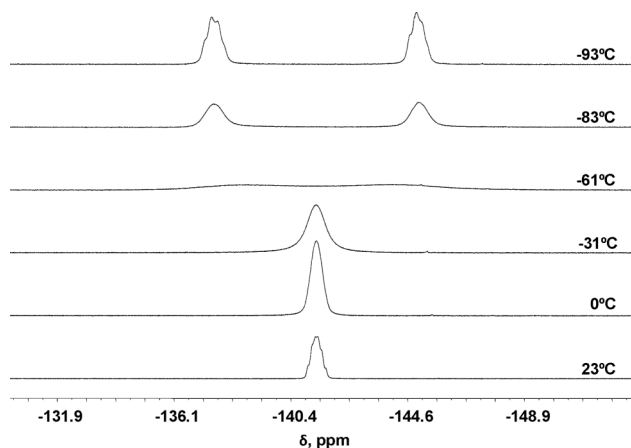


Fig. 4 ^{19}F NMR (470.1 MHz) spectra of **6** in CD_2Cl_2 at temperatures between 23 °C and -93 °C.

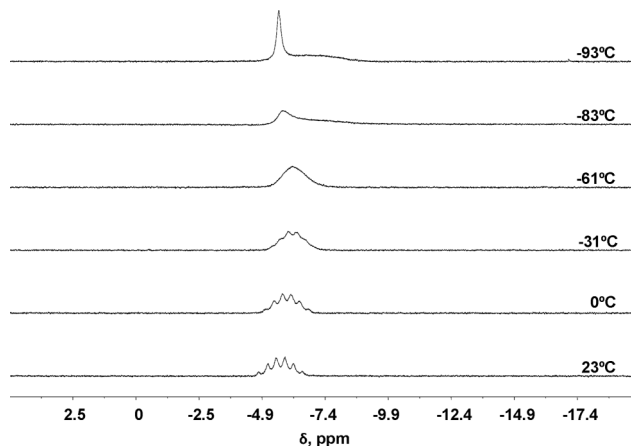


Fig. 5 $^{31}\text{P}\{^1\text{H}\}$ NMR (202.3 MHz) spectra of **6** in CD_2Cl_2 at temperatures between 23 °C and -93 °C.

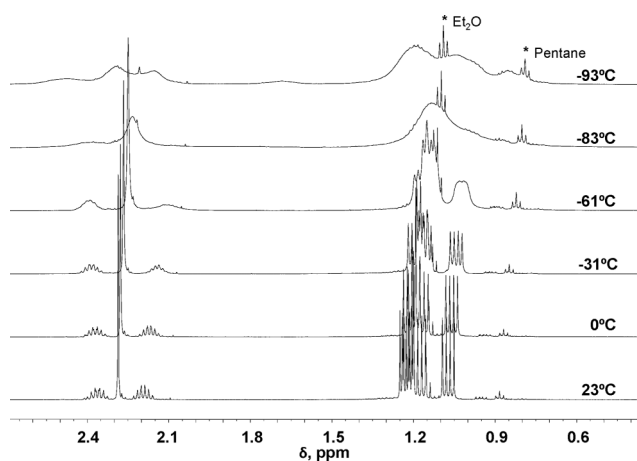


Fig. 6 The aliphatic area of the ^1H NMR (500 MHz) spectra of **6** in CD_2Cl_2 at temperatures between $23\text{ }^\circ\text{C}$ and $-93\text{ }^\circ\text{C}$.

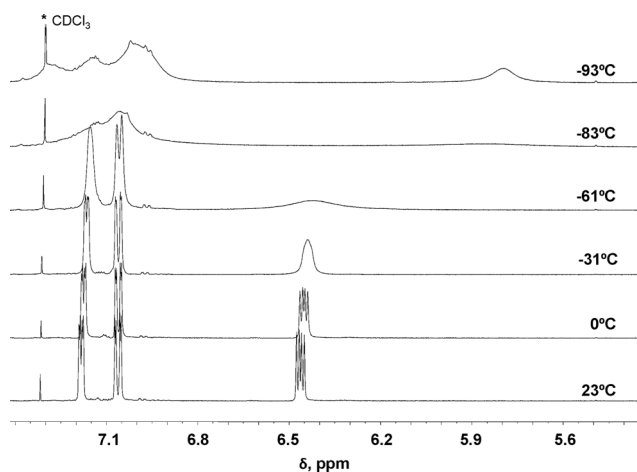


Fig. 7 The aromatic area of the ^1H NMR (500 MHz) spectra of **6** in CD_2Cl_2 at temperatures between $23\text{ }^\circ\text{C}$ and $-93\text{ }^\circ\text{C}$.

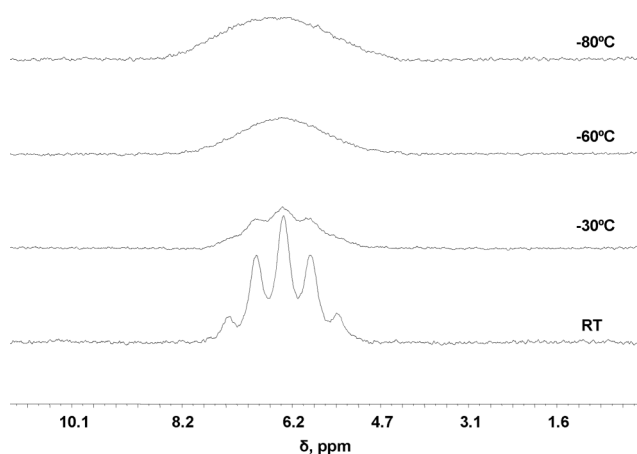


Fig. 8 $^{11}\text{B}\{^1\text{H}\}$ NMR (128.2 MHz) spectra of **6** in CD_2Cl_2 at temperatures between RT and $-80\text{ }^\circ\text{C}$.

Analysis of the exchange process

We propose that the spectroscopic observations are best accounted for by a fast equilibrium between two degenerate four-coordinate boron structures (Scheme 2). This transformation can be plausibly

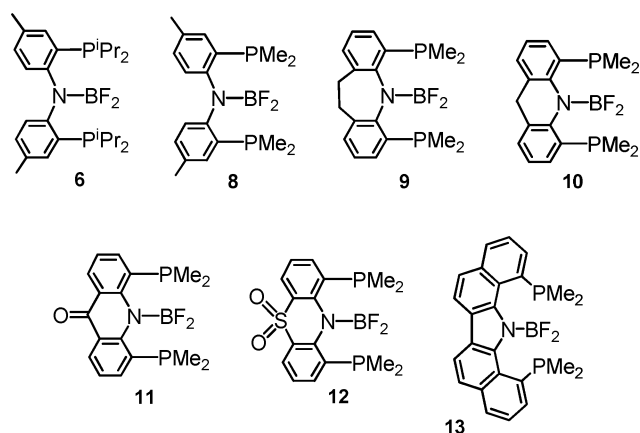


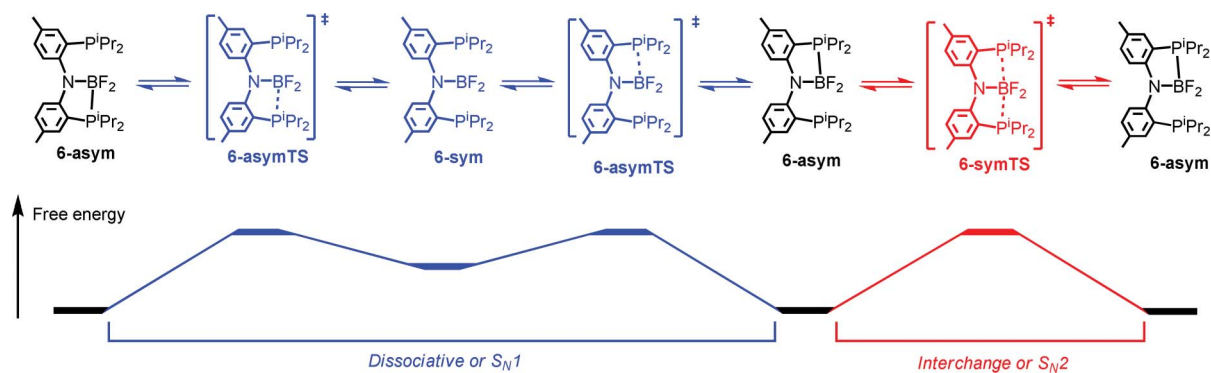
Fig. 9 Drawings of the different (PNP*) BF_2 compounds that were analyzed computationally.

accomplished either through interchange, in a degenerative $\text{S}_{\text{N}}2$ displacement of one P by the other, or dissociatively, *via* a three-coordinate intermediate **6-sym**. Experimentally, we cannot distinguish between the two alternatives, but our computational studies (*vide infra*) attempt to address this issue. We briefly considered that the exchange process may involve an ionic $[(\text{PNP})\text{BF}]^+[\text{F}]^-$ ground state and exchange between the bound and free fluoride. This hypothesis was ruled out because (a) neither ^{19}F NMR resonance at low temperature matched the chemical shift expected for free fluoride;³⁷ (b) it would not explain the different coupling experienced by the two ^{31}P nuclei; and (c) it was in contradiction with the similar coupling experienced by the two ^{19}F nuclei, judging by the fine structure of the low temperature resonances. Analysis of the line shapes in the ^{19}F and ^1H NMR spectra (decoalescence of the resonance appearing at δ 6.47 ppm at $23\text{ }^\circ\text{C}$) as a function of temperature allowed determination of the activation parameters for the exchange process. Using gNMR software,³⁸ we obtained $\Delta H^\ddagger = 8.1(3)\text{ kcal mol}^{-1}$ and $\Delta S^\ddagger = -6.0(15)\text{ eu}$ values. From these values, ΔG^\ddagger at 298 K was calculated to be $9.9(5)\text{ kcal mol}^{-1}$.

Computational studies of (PNP) BF_2 (**6**)

The computed ground state structure for **6** (**6-asym** in Scheme 2) is a good match for the experimentally determined solid-state structure. The bonding B–N and B–F distances are within 0.01 \AA and the calculated B–P bond length is only 0.03 \AA longer. The non-bonded B \cdots P distance in the calculation (*ca.* 3.96 \AA) is shorter than in the X-ray structure (*ca.* 4.35 \AA), but it is still far too long to be considered within bonding range and the lone pair of P is not oriented towards B. The disparity is primarily due to a different twist angle about the N–C bond for the aryl ring carrying the “free” phosphine. We would not expect this conformational change to be modeled precisely with DFT, especially when comparing the gas-phase DFT model to the experimental structure in the crystal.

We were also able to locate a C_2 symmetric structure **6-sym** (Fig. 10). It is not a transition state (TS), but rather a local minimum lying 4.9 kcal mol^{-1} above the ground state in free energy. Although it is symmetric, with equal B–P distances, this structure is best described as *three-coordinate* at B rather than *five-coordinate*. The B–P distances are $>3\text{ \AA}$ and the apparent directionality of the lone pair on each P is not aligned with the



Scheme 2 Plausible mechanisms for the exchange process in **6**. The -sym/-asm and -symTS/-asmTS notation is also used in the text for the analogous structures of other (PNP*)BF₂ compounds.

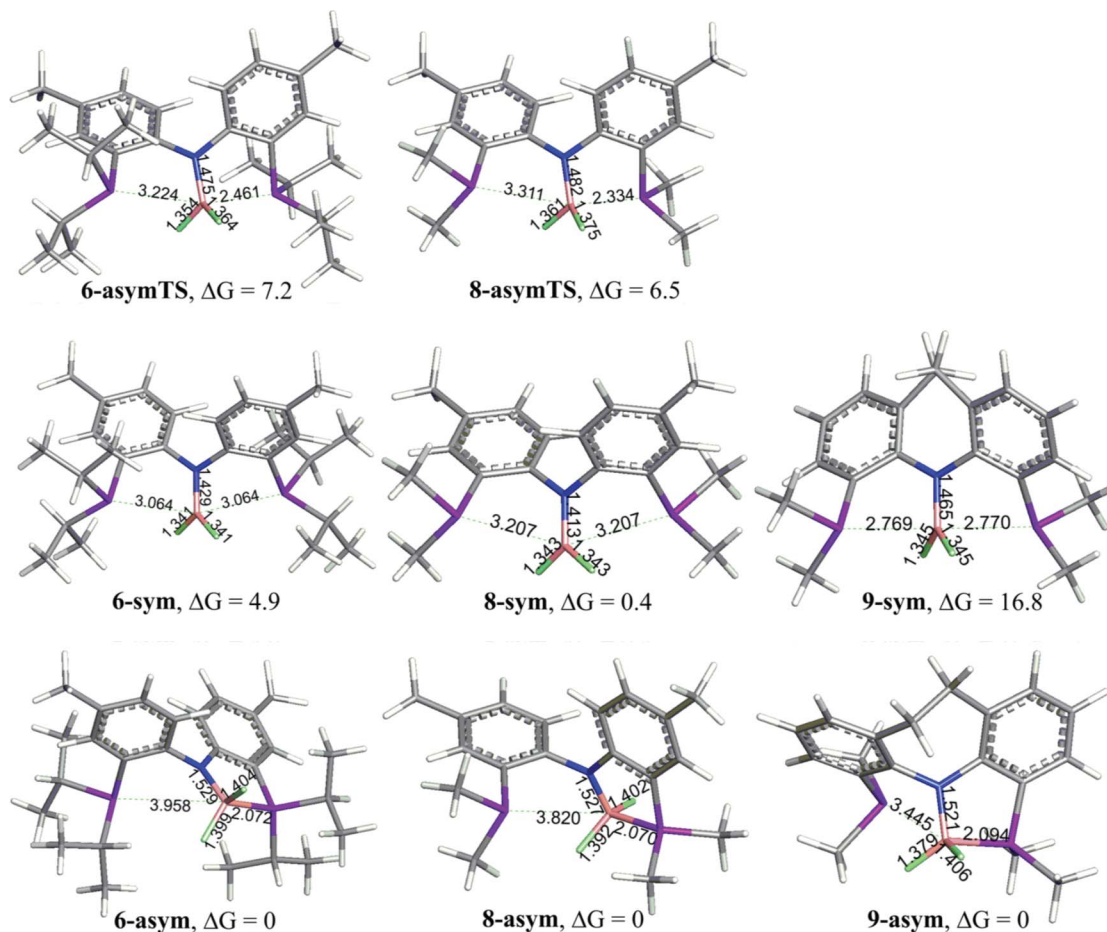


Fig. 10 The calculated minima and TS for compounds **6**, **8**, and **9**. The ΔG values are in kcal mol⁻¹ and are relative to the asm structure, set at 0 separately for each formulation.

boron atom.³⁹ At the same time, the B–F and especially the B–N distances are greatly shortened compared to **6-asm**, and the BF₂ unit twists to become nearly coplanar with the plane of the trigonal planar N (C–N–B–F dihedral angle of *ca.* 25° in **6-sym** vs. *ca.* 70° in **6-asm**). All of this indicates that the empty orbital at B in **6-sym** is not stabilized by donation from P, but rather by enhanced π -donation from the two F atoms and especially the N atom.

We did locate the TS (**6-asmTS**) for the interconversion between **6-sym** and **6-asm**. It was calculated to be 7.2 kcal mol⁻¹

above the ground state in free energy. Not surprisingly, its geometry is intermediate between **6-sym** and **6-asm**. Given that the longer B–P distance in it is >3.2 Å, **6-asmTS** is more appropriately viewed as an S_N1-like TS for the dissociation of a phosphine rather than an S_N2-like TS for concerted displacement of one phosphine by another. The overall dynamic process for **6** thus can be described as an S_N1-like process (Scheme 2).

The calculated activation parameters for the exchange process in **6** ($\Delta H^\ddagger = 5.9$ kcal mol⁻¹ and $\Delta S^\ddagger = -4.6$ eu) do not greatly

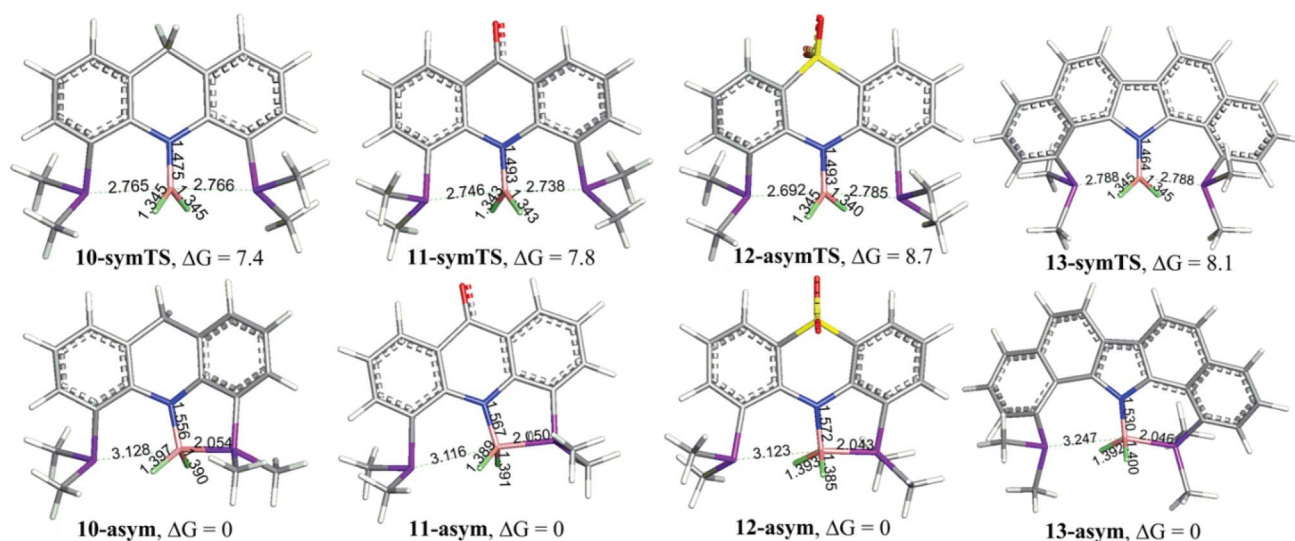


Fig. 11 The calculated minima and TS for compounds **10–13**. The ΔG values are in kcal mol^{-1} and are relative to the asym structure set at 0, separately for each formulation.

differ from the experimentally obtained ones ($\Delta H^\ddagger = 8.1(3)$ kcal mol^{-1} and $\Delta S^\ddagger = -6.0(15)$ eu). Our calculations were performed for gas phase molecules, which may partially explain the slight discrepancy in enthalpy of activation. In addition, the energy profile for this exchange is quite shallow and the optima may be difficult to capture computationally with true precision. In order to test the validity of our computational approach on another system, we have used DFT to analyze the structure of Akiba and Yamamoto's compound **3**. A 10-B-5 minimum structure was located,⁴⁰ in accord with Akiba and Yamamoto's structural and theoretical studies of **3**.²¹

Computational studies of analogs of (PNP)BF₂ (**6**)

Besides the model of experimentally studied **6**, we also undertook a DFT study of the BF₂ derivatives of six other PNP ligands (Fig. 9). First, we performed calculations on a system with a PNP ligand that bears PMe₂ donor arms (**8**, Fig. 10). We wondered if smaller phosphine donors might lower the energy of a five-coordinate species. We did not find any minimum, however, that can be described as five-coordinate at B. The overall situation is in fact fully analogous to the P'Pr₂-containing ligand. The free energy of the symmetric structure **8-sym** was indeed lowered to the point that it is essentially isoergic with the four-coordinate dissymmetric ground state structures but this is not due to improved interactions with P donors. On the contrary, the B–P distances in **8-sym** are *ca.* 0.14 Å longer than in **6-sym**, while the B–N distance is slightly shorter. Thus, it appears that the smaller phosphines in **8** lead to a lower energy for the symmetric isomer because the smaller phosphine size allows for greater conformational flexibility in the molecule and allows the phosphines to interfere less with the establishment of the conformation that maximizes the π -bonding overlap between the N and B orbitals. The transition state **8-asymTS** is similar in energy and in approximate geometry to that of **6-asymTS**.

We also considered whether a PNP ligand with a more rigidly constructed backbone might favor the hypercoordinate structure.

We previously reported⁴¹ Pd, Rh, and Ir complexes of the “tied” PNP ligand (with P'Pr₂ arms) where the two aromatic rings are linked (“tied”) by a CH₂CH₂ fragment. Here, we used DFT calculations to analyze the BF₂ derivative of this ligand with PMe₂ arms (**9**, Fig. 10). In addition to the CH₂CH₂ linker, we also performed computational analyses of the BF₂ derivatives with “tied” PNP ligands that contain CH₂ (**10**), CO (**11**), and SO₂ (**12**) bridges (Fig. 11). A BF₂ derivative of an even more rigid PNP ligand **13** was also studied (Fig. 11). None of the compounds **9–13** were prepared experimentally. All the “tied” ligands here were studied with PMe₂ donor arms and the ligands in compounds **10–13** have not been made experimentally with any phosphine donors.

Two different minima were again found for **9**, a dissymmetric minimum **9-asym** (or, rather, two degenerate ones) and a symmetric **9-sym**. Remarkably, **9-asym** was 16.8 kcal mol^{-1} higher in free energy than **9-sym** – a dramatic difference compared to the nearly isoergic conformations of the “untied” analogs for **8**. **9-sym** featured shorter B–P distances than **8-sym** (2.77 Å vs. 3.21 Å) but the N–B distance was markedly longer. Additionally, the coordination planes around B and N are not nearly as close to coplanarity as in **8-sym**. It appears that the “tied” ligand in **9** forces a coordination environment about B that inches closer to five-coordinate, although the B–P distances of 2.77 Å are still quite long (*ca.* 0.7 Å longer than the true single B–P bond in the solid-state structure of **6** (*i.e.*, **6-asym**)). However, this enforcement is clearly less stabilizing than the π -donation from N in **6-sym** or **8-sym**. In fact, it is likely that the more rigid “tied” ligand in **9** simply experiences a great deal of conformational strain attempting to adopt the most stabilized three-coordinate geometry at B. We did not look for the TS in **9** as they would clearly be even higher in energy than **9-asym**.

With compounds **10–13**, the calculated situation was slightly different. The symmetric structures for **10**, **11**, and **13** were not minima but rather TS (**10-symTS**, **11-symTS**, **13-symTS**). The TS for **12** (**12-asymTS**) was modestly dissymmetric, and with several attempts the truly symmetric structure was not located. Remarkably, the free energies of these four TS were very similar

to each other, and to that of **8-asymTS**, ranging only from 6.5 to 8.7 kcal mol⁻¹. The metric parameters of the TS for **10–13** were also rather similar to **8-asymTS**, with B–P distances on the order of 2.7–2.8 Å. With CO (**11**) and SO₂ (**12**) linkers, we sought to examine whether an electron-withdrawing substituent can attenuate the π -donating ability of N towards B and destabilize the three-coordinate structure. The B–N bond is indeed slightly elongated for **11-symTS** and **12-asymTS**, indicative of decreased π -donation from N, but apparently this is not a very important effect.

The distinction between S_N1 and S_N2 pathways boils down to whether the symmetric structure is a minimum or a transition state. In the (PNP)BF₂ systems under study, this distinction is rather slight, amounting to a few kcal mol⁻¹ at the most. In fact, what we see is essentially a continuum of reaction coordinate profiles, with the transition state being more or less symmetric. In none of the computed structures, be they transition state or minima, do we see two reasonably short B–P bonds interpretable as a 10-B-5 structure. It appears that the stabilization of the symmetric geometry relies largely on the enhanced π -donation from the fluorides or the amido and not on the dual donation from the phosphine arms.

These observations dovetail the conclusions of Akiba, Yamamoto *et al.* in that 10-B-5 (and 10-C-5) minima are only accessible when a trigonal planar 6-B-3 core is complemented by two weak axial donors that do not form strong two-center, two-electron bonds. It is possible that the choice of both phosphines as side arms and of the central anchoring amido is counterproductive in the search of a 10-B-5 structure. A phosphine may be too strong a donor, forming a classical two-center, two-electron bond too strongly, while the amido is too stabilizing of a 6-B-3 structure *via* additional π -donation.

Conclusions

Utilization of a diarylamido/bis(phosphine) PNP ligand to access a symmetric and hypercoordinate 10-B-5 compound (PNP)BF₂ (**6**) did not prove successful. The ground state structure of **6** was determined to be a classical, dissymmetric 8-B-4 variant with one non-coordinated phosphine in both solution and solid state. The interconversion between the two 8-B-4 forms is a net degenerate displacement of one phosphine arm by the other. This process took place with only a small activation barrier ($\Delta H^\ddagger = 8.1(3)$ kcal mol⁻¹ and $\Delta S^\ddagger = -6.0(15)$ eu) in solution.

A DFT computational study of the exchange process considered two possible mechanisms: (a) a dissociative or S_N1-like mechanism with the dissociation of one phosphine preceding the coordination of the other and (b) an interchange or S_N2-like mechanism with a concerted displacement of the departing phosphine by the incoming one. This computational study analyzed several related (PNP)BF₂ systems along with the exact compound obtained experimentally (**6**). The other (PNP)BF₂ systems differed from **6** in the substituents on the phosphine arms (PMe₂ *vs.* P^tPr₂) and in the rigidity of the pincer backbone. For **6**, calculations indicated an S_N1-like mechanism, while for some others, an S_N2-like mechanism was evident. The distinction between the two is slight and the changes in the pincer ligand could not bring about a stable 10-B-5 minimum.‡

Experimental

General considerations

Unless otherwise noted, all manipulations and reactions were performed under argon, using standard glove box and Schlenk line techniques. Diethyl ether, toluene, pentane, and C₆D₆ were dried over and distilled from NaK/Ph₂CO/18-crown-6 and stored over molecular sieves in an Ar-filled glove box. CD₂Cl₂ was dried over CaH₂, vacuum transferred and stored over molecular sieves in an Ar-filled glove box. Me(PNP)H (**1**) was prepared according to the literature procedure.¹ All other chemicals were used as received from commercial vendors. NMR spectra were recorded on a Varian iNova 300 (¹H NMR, 299.951 MHz; ¹³C NMR, 75.426 MHz; ³¹P NMR, 121.422 MHz; ¹⁹F NMR, 282.211 MHz), Varian NMRS 500 (¹H NMR, 499.682 MHz; ¹³C NMR, 125.660 MHz; ³¹P NMR, 202.265 MHz; ¹⁹F NMR, 470.111 MHz) and Varian iNova 400 (¹¹B NMR, 128.191 MHz). Chemical shifts are reported in δ (ppm). For ¹H and ¹³C NMR, the residual solvent peak was used to reference the spectra. ³¹P NMR spectra were referenced using 85% H₃PO₄ at δ 0 ppm. ¹⁹F NMR spectra were referenced using CF₃CO₂H at δ -78.5 ppm. ¹¹B NMR spectra were referenced using Et₂OBF₃ at δ 0 ppm. Elemental analysis was performed by Complete Analysis Laboratories Inc., Parsippany, NJ, USA.

Computational details

All calculations were performed with the Gaussian03 program.⁴² The B3LYP^{43–45} density functional was used for all geometry optimization and frequency calculation with LANL2DZdp⁴⁶ with effective core potential (ECP) was used for P and S; 6-31++G(d,p)^{47–49} was used for B, F, N, and O in direct contact with B; 6-31G(d)^{47–49} was used for other O and all C and H. All structures were fully optimized with default convergence criteria, and frequencies were calculated to ensure that there was no imaginary frequency for minima. Zero point energies and thermodynamic functions were calculated at 298.15 K and 1 atm.

X-ray crystallography

All operations were performed on a Bruker-Nonius Kappa Apex2 diffractometer, using graphite-monochromated Mo-K α radiation. All diffractometer manipulations, including data collection, integration, scaling, and absorption corrections were carried out using the Bruker Apex2 software.⁵⁰ **Compound 6**: Preliminary cell constants were obtained from three sets of 12 frames. Data collection was carried out at 120 K, using a frame time of 40 s and a detector distance of 60 mm. The optimized strategy used for data collection consisted of three phi and one omega scan sets, with 0.5° steps in phi or omega; completeness was 99.8%. A total of 1810 frames were collected. Final cell constants were obtained from the *xyz* centroids of 3474 reflections after integration. From the systematic absences and the observed metric constants and intensity statistics, space group *P2₁/c* was chosen initially; subsequent solution and refinement confirmed the correctness of this choice. The structure was solved using *SIR92*,⁵¹ and refined (full-matrix-least squares) using the Oxford University *Crystals for Windows* program.⁵² All ordered non-hydrogen atoms were refined using anisotropic displacement parameters. After location

of H atoms on electron-density difference maps, the H atoms were initially refined with soft restraints on the bond lengths and angles to regularise their geometry (C—H in the range 0.93–0.98 Å and U_{iso} (H) in the range 1.2–1.5 times U_{eq} of the parent atom), after which the positions were refined with riding constraints.⁵³ Crystals of the compound exhibited weak diffraction patterns, with a steep descent in intensity beyond $d = 1.0$ Å. Most data beyond that resolution was rather weak. Nonetheless, the structure itself was unequivocally determined. There was no ambiguity regarding atom types or stereochemistry. The final least-squares refinement converged to $R_1 = 0.0515$ ($I > 2\sigma(I)$, 3497 data) and $wR_2 = 0.1584$ (F^2 , 5110 data, 289 parameters). The final CIF is available as supporting material.† **Compound 7**: Preliminary cell constants were obtained from three sets of 12 frames. Data collection was carried out at 120 K, using a frame time of 30 s and a detector distance of 60 mm. The optimized strategy used for data collection consisted of two phi and two omega scan sets, with 0.5° steps in phi or omega; completeness was 99.6%. A total of 1776 frames were collected. Final cell constants were obtained from the xyz centroids of 6591 reflections after integration. From the systematic absences and the observed metric constants and intensity statistics, space group $P2_1/c$ was chosen initially; subsequent solution and refinement confirmed the correctness of this choice. The structure was solved using *SIR92*,⁵¹ and refined (full-matrix-least squares) using the Oxford University *Crystals for Windows* program.⁵² All ordered non-hydrogen atoms were refined using anisotropic displacement parameters. After location of H atoms on electron-density difference maps, the H atoms were initially refined with soft restraints on the bond lengths and angles to regularize their geometry (C—H in the range 0.93–0.98 Å and U_{iso} (H) in the range 1.2–1.5 times U_{eq} of the parent atom), after which the positions were refined with riding constraints.⁵³ Crystals of the compound exhibited weak diffraction patterns, with a sharp cutoff at *ca.* $d = 1.0$ Å. Significant data beyond that resolution was not attainable. Nonetheless, the structure itself was unequivocally determined. There was no ambiguity regarding atom types or stereochemistry. The final least-squares refinement converged to $R_1 = 0.0364$ ($I > 2\sigma(I)$, 2592 data) and $wR_2 = 0.0892$ (F^2 , 3108 data, 334 parameters). The final CIF is available as supporting material.† CheckCIF displayed two Alert A items, related to the low resolution issues described above. Accordingly, a similar explanation appears as a validation reply form item in the CIF and CheckCIF.†

Preparations

(PNP)BF₂ (6). In an Ar-filled glove box, (PNP)H (**4**) (587 mg, 1.37 mmol) was dissolved in toluene. ⁿBuLi (0.6 mL of 2.5 M soln in hexane, 1.5 mmol) was added *via* a syringe and the solution immediately became a clear, bright yellow. After stirring for 10 min, the Schlenk flask was covered with foil to minimize light exposure and Me₂SBF₃ (143 μL, 1.36 mmol) was added. The solution became a cloudy, pale yellow. The reaction solution was stirred overnight, then volatiles were removed *in vacuo* and the solution was filtered through a pad of Celite using Et₂O. The Et₂O solution was layered with pentane, and the flask was placed in the freezer at -35°C . While trying to minimize light exposure, the white solid was collected over a glass frit, washed several times with pentane then dried, yielding 428 mg (66% yield) of the isolated

product. *Without protection from ambient light, some formation (<5% by NMR) of unidentified impurities was observed. Leaving a pure C₆D₆ solution of 6 on a windowsill exposed to sunlight for 12 h also resulted in minor decomposition (<5% by NMR).* ¹H NMR (C₆D₆): δ 7.08 (dd, 2H, $J = 1.5$ Hz, $J = 4.5$ Hz, Ar–H), 6.95 (dd, 2H, $J = 2.5$ Hz, $J = 8.5$ Hz, Ar–H), 6.83 (dd, 2H, $J = 5$ Hz, $J = 8.5$ Hz, Ar–H), 2.13 (s, 6H, –CH₃), 2.07 (m, 2H, $J = 7$ Hz, –CH(CH₃)₂), 2.03 (m, 2H, $J = 7$ Hz, –CH(CH₃)₂), 1.23 (dd, 6H, $J = 7.5$ Hz, $J = 14$ Hz, –CH(CH₃)₂), 1.17 (dd, 6H, $J = 7$ Hz, $J = 14$ Hz, –CH(CH₃)₂), 1.08 (dd, 6H, $J = 7.5$ Hz, $J = 15$ Hz, –CH(CH₃)₂), 0.99 (dd, 6H, $J = 7.5$ Hz, $J = 14.5$ Hz, –CH(CH₃)₂). ³¹P{¹H} NMR (C₆D₆): δ –6.5 (br m). ¹⁹F NMR (C₆D₆): δ –139.3 (br m). ¹¹B{¹H} NMR (C₆D₆): δ 6.4 (br m). ¹H NMR (CD₂Cl₂): δ 7.19 (dd, 2H, $J = 2$ Hz, $J = 5$ Hz, Ar–H), 7.07 (dd, 1H, $J = 2$ Hz, $J = 8$ Hz, Ar–H), 6.47 (dd, 2H, $J = 4$ Hz, $J = 7.5$ Hz, Ar–H), 2.37 (m, 2H, $J = 8$ Hz, –CH(CH₃)₂), 2.29 (s, 6H, –CH₃), 2.20 (m, 2H, $J = 7$ Hz, –CH(CH₃)₂), 1.23 (dd, 6H, $J = 7.5$ Hz, $J = 15$ Hz, –CH(CH₃)₂), 1.22 (dd, 6H, $J = 7.5$ Hz, $J = 14$ Hz, –CH(CH₃)₂), 1.18 (dd, 6H, $J = 7.5$ Hz, $J = 15$ Hz, –CH(CH₃)₂), 1.08 (dd, 6H, $J = 7$ Hz, $J = 14$ Hz, –CH(CH₃)₂). ¹³C{¹H} NMR (CD₂Cl₂): δ 152.1 (t, $J_{\text{P-C}} = 17$ Hz, Ar), 133.3 (Ar), 132.8 (Ar), 130.4 (Ar), 121.8 (Ar), 121.1 (Ar), 24.0 (d, $J = 7$ Hz), 21.8 (d, $J = 8$ Hz), 20.8 (ArMe), 19.7 (d, $J = 7.3$ Hz), 19.3 (d, $J = 7.3$ Hz), 19.2 (d, $J_{\text{P-C}} = 12$ Hz, –CHMe₂), 18.3 (d, $J = 5$ Hz). ³¹P{¹H} NMR (CD₂Cl₂): δ –5.6 (br m, $J_{\text{P-B}} = 68 \pm 4$ Hz, $J_{\text{P-F}} = 72$ Hz \pm 4 Hz). ¹⁹F NMR (CD₂Cl₂): δ –141.3 (br m, $J_{\text{F-B}} = 55 \pm 5$ Hz, $J_{\text{F-F}} = 75 \pm 5$ Hz). ¹¹B{¹H} NMR (CD₂Cl₂): δ 6.4 (br m, $J_{\text{P-B}} = 57 \pm 2$ Hz, $J_{\text{P-B}} = 69 \pm 2$ Hz). *NMR data for 6 at low temperature:* ¹¹B{¹H} NMR (CD₂Cl₂, -80°C): δ 6.4 (br s); ³¹P{¹H} NMR (CD₂Cl₂, -93°C): δ –5.7 (s), –7.0 (br s); ¹⁹F NMR (CD₂Cl₂, -93°C): δ –138 (br m), –145 (br m); ¹H NMR (CD₂Cl₂, -93°C): δ 7.29, 7.15, 7.00 (3 broad, overlapping signals, Ar–H), 5.8 (br s, Ar–H), 2.47, 2.29, 2.21, 2.15 (4 overlapping signals, 3 broad with sharper signal at 2.21), 1.7 (br s), 1.19, 1.04, 0.85 (3 broad, overlapping signals). Elemental analysis, calculated (found) for C₂₆H₄₀NP₂BF₂: C, 65.37 (65.42); H, 8.45 (8.34).

Acknowledgements

Support of this research by the Petroleum Research Fund (grant 44904-AC3), the Welch Foundation (grant A-1717), the Alfred P. Sloan Foundation (Research Fellowship to O.V.O.), the Dreyfus Foundation (Camille Dreyfus Teacher-Scholar Award to O.V.O.) is gratefully acknowledged. We also thank the National Science Foundation for the partial support of this work through grant CHE-0521047 for the purchase of a new X-ray diffractometer at Brandeis University. We are grateful to Prof. Lori Watson for initial computational work and to Jeremy Heyman and Mayank Puri for initial work on the solution of the solid-state structure of **6**. We thank Prof. Michael Hall (Texas A&M) for helpful discussions and to the Supercomputing Facility and the Laboratory for Molecular Simulation at Texas A&M University for computer time and software.

Notes and references

- (a) L.-C. Liang, J.-M. Lin and C.-H. Hung, *Organometallics*, 2003, **22**, 3007; (b) A. M. Winter, K. Eichele, H.-G. Mack, S. Potuznik, H. A. Mayer and W. C. Kaska, *J. Organomet. Chem.*, 2003, **682**, 149.
- L. Fan, B. M. Foxman and O. V. Ozerov, *Organometallics*, 2004, **23**, 326.

- 3 (a) L.-C. Liang, *Coord. Chem. Rev.*, 2006, **250**, 1152; (b) O. V. Ozerov, in *The Chemistry of Pincer Compounds*, ed. D. Morales-Morales and C. Jensen, Elsevier, Amsterdam, 2007, pp 287–309; (c) D. J. Mindiola, *Acc. Chem. Res.*, 2006, **39**, 813.
- 4 D. Bacciu, C.-H. Chen, P. Surawatanawong, B. M. Foxman and O. V. Ozerov, *Inorg. Chem.*, 2010, **49**, 5328.
- 5 J. C. DeMott, C. Guo, B. M. Foxman, D. V. Yandulov and O. V. Ozerov, *Mendeleev Commun.*, 2007, **17**, 63.
- 6 C. W. Perkins, J. C. Martin, A. J. Arduengo, W. Lau, A. Alegria and J. K. Kochi, *J. Am. Chem. Soc.*, 1980, **102**, 7753 N is the number of valence electrons about an atom X, and L is the number of ligands directly bound to X.
- 7 “Hypercoordinate”⁸ is an alternative term to the commonly used “hypervalent”^{9–11} for description of compounds which possess higher coordination numbers than the octet rule would predict possible. The contradiction between the intended meaning of “hypervalent” and the meaning of “valence” has been discussed elsewhere^{12–15}.
- 8 (a) D. Kost and I. Kalikhman, *Acc. Chem. Res.*, 2009, **42**, 303; (b) E. Brendler, E. Wchtler and J. Wagler, *Organometallics*, 2009, **28**, 5459; (c) D. L. Cooper, T. P. Cunningham, J. Gerratt, P. B. Karadakov and M. Raimondi, *J. Am. Chem. Soc.*, 1994, **116**, 4414.
- 9 J. I. Musher, *Angew. Chem., Int. Ed. Engl.*, 1969, **8**, 54.
- 10 K.-y. Akiba, *Chemistry of Hypervalent Compounds*, Wiley-VCH, New York, 1999.
- 11 (a) A. E. Reed and P. V. R. Schleyer, *J. Am. Chem. Soc.*, 1990, **112**, 1434; (b) T. Cleveland and C. R. Landis, *J. Am. Chem. Soc.*, 1996, **118**, 6020; (c) S. Noury, B. Silvi and R. J. Gillespie, *Inorg. Chem.*, 2002, **41**, 2164.
- 12 W. B. Jensen, *J. Chem. Educ.*, 2006, **83**, 175.
- 13 D. W. Smith, *J. Chem. Educ.*, 2005, **82**, 1202.
- 14 R. J. Gillespie and B. Silvi, *Coord. Chem. Rev.*, 2002, **233–234**, 53.
- 15 G. Parkin, *J. Chem. Educ.*, 2006, **83**, 791.
- 16 K. Yurkerwich and G. Parkin, *Inorg. Chim. Acta*, 2010, **364**, 157.
- 17 J. C. DeMott, F. Basuli, U. J. Kilgore, B. M. Foxman, J. C. Huffman, O. V. Ozerov and D. J. Mindiola, *Inorg. Chem.*, 2007, **46**, 6271.
- 18 S. Pierrefixe, C. F. Guerra and F. M. Bickelhaupt, *Chem.–Eur. J.*, 2008, **14**, 819.
- 19 K.-y. Akiba, M. Yamashita, Y. Yamamoto and S. Nagase, *J. Am. Chem. Soc.*, 1999, **121**, 10644.
- 20 M. Yamashita, Y. Yamamoto, K.-y. Akiba and S. Nagase, *Angew. Chem., Int. Ed.*, 2000, **39**, 4055.
- 21 M. Yamashita, Y. Yamamoto, K.-y. Akiba, D. Hashizume, F. Iwasaki, N. Takagi and S. Nagase, *J. Am. Chem. Soc.*, 2005, **127**, 4354.
- 22 M. Yamashita, K. Watanabe, Y. Yamamoto and K.-y. Akiba, *Chem. Lett.*, 2001, 1104–1105.
- 23 M. Yamashita, K. Kamura, Y. Yamamoto and K.-y. Akiba, *Chem.–Eur. J.*, 2002, **8**, 2976.
- 24 M. Yamashita, Y. Mita, Y. Yamamoto and K.-y. Akiba, *Chem.–Eur. J.*, 2003, **9**, 3655.
- 25 J.-y. Nakatsuji and Y. Yamamoto, *Bull. Chem. Soc. Jpn.*, 2010, **83**, 767.
- 26 T. Yano, T. Yamaguchi and Y. Yamamoto, *Chem. Lett.*, 2009, **38**, 794.
- 27 (a) R. Breslow, S. Garratt, L. Kaplan and D. LaFollette, *J. Am. Chem. Soc.*, 1968, **90**, 4051; (b) R. Breslow, L. Kaplan and D. LaFollette, *J. Am. Chem. Soc.*, 1968, **90**, 4056; (c) R. J. Basalay and J. C. Martin, *J. Am. Chem. Soc.*, 1973, **95**, 2565; (d) J. C. Martin and R. J. Basalay, *J. Am. Chem. Soc.*, 1973, **95**, 2572; (e) T. R. Forbus Jr. and J. C. Martin, *J. Am. Chem. Soc.*, 1979, **101**, 5057; (f) J. C. Martin, *Science*, 1983, **221**, 509; (g) M. Hojo, T. Ichi and K. Shibato, *J. Org. Chem.*, 1985, **50**, 1478; (h) S. Toyota, T. Futawaka, H. Ikeda and M. Oki, *J. Chem. Soc., Chem. Commun.*, 1995, 2499.
- 28 (a) *The Chemistry of Pincer Compounds*, ed. D. Morales-Morales, C. Jensen, Elsevier, Amsterdam, 2007; (b) M. E. van der Boom and D. Milstein, *Chem. Rev.*, 2003, **103**, 1759.
- 29 W. Weng, L. Yang, B. M. Foxman and O. V. Ozerov, *Organometallics*, 2004, **23**, 4700.
- 30 H. J. Reich, WinDNMR: *NMR Spectrum Calculations Version 7.1.13*, 2008.
- 31 ORTEP plots were created using *Ortep-3 for Windows* L. Farugia, *J. Appl. Crystallogr.*, 1997, **30**, 565.
- 32 (a) M. Yamashita, Y. Aramaki and K. Nozaki, *New J. Chem.*, 2010, **34**, 1774; (b) I. J. Arroyo, R. Hu, G. Merino, B. Z. Tang and E. Peña-Cabrera, *J. Org. Chem.*, 2009, **74**, 5719; (c) K. Tram, H. Yan, H. A. Jenkins, S. Vassiliev and D. Bruce, *Dyes Pigm.*, 2009, **82**, 392.
- 33 U. Monkowius, S. Nogai and H. Schmidbaur, *Dalton Trans.*, 2003, 987.
- 34 C. Loschen, K. Voigt, J. Frunzke, A. Diefenbach, M. Diedenhofen and G. Frenking, *Z. Anorg. Allg. Chem.*, 2002, **628**, 1294.
- 35 T. A. Ford, *J. Phys. Chem. A*, 2008, **112**, 7296.
- 36 (a) G. C. Welch, R. Prieto, M. A. Dureen, A. J. Lough, O. A. Labeodan, T. Höltrichter-Rössmann and D. W. Stephan, *Dalton Trans.*, 2009, 1559; (b) P. Spies, R. Fröhlich, G. Kehr, G. Erker and S. Grimme, *Chem.–Eur. J.*, 2008, **14**, 333; (c) D. C. Bradley, M. B. Hursthouse, M. Motevalli and D. H. Zheng, *J. Chem. Soc., Chem. Commun.*, 1991, 7.
- 37 (a) H. Sun and S. G. DiMugno, *J. Am. Chem. Soc.*, 2005, **127**, 2050; (b) A. Kornath, F. Neumann and H. Oberhammer, *Inorg. Chem.*, 2003, **42**, 2894; (c) K. O. Christe, W. W. Wilson, R. D. Wilson, R. Bau and J. A. Feng, *J. Am. Chem. Soc.*, 1990, **112**, 7619.
- 38 P. H. M. Budzelaar, gNMR: *NMR Simulation Program Version 5.0.6.0*, 2006.
- 39 See Fig. S28 in the ESI.
- 40 See the ESI for details of our calculations.
- 41 (a) W. Weng, C. Guo, R. Çelenigil-Çetin, B. M. Foxman and O. V. Ozerov, *Chem. Commun.*, 2006, 197; (b) W. Weng, C. Guo, C. P. Moura, L. Yang, B. M. Foxman and O. V. Ozerov, *Organometallics*, 2005, **24**, 3487.
- 42 M. J. Frisch, G. W. Trucks, H. B. Schlegel, G. E. Scuseria, M. A. Robb, J. R. Cheeseman, J. A. Montgomery Jr., T. Vreven, K. N. Kudin, J. C. Burant, J. M. Millam, S. S. Iyengar, J. Tomasi, V. Barone, B. Mennucci, M. Cossi, G. Scalmani, N. Rega, G. A. Petersson, H. Nakatsuji, M. Hada, M. Ehara, K. Toyota, R. Fukuda, J. Hasegawa, M. Ishida, T. Nakajima, Y. Honda, O. Kitao, H. Nakai, M. Klene, X. Li, J. E. Knox, H. P. Hratchian, J. B. Cross, V. Bakken, C. Adamo, J. Jaramillo, R. Gomperts, R. E. Stratmann, O. Yazyev, A. J. Austin, R. Cammi, C. Pomelli, J. W. Ochterski, P. Y. Ayala, K. Morokuma, G. A. Voth, P. Salvador, J. J. Dannenberg, V. G. Zakrzewski, S. Dapprich, A. D. Daniels, M. C. Strain, O. Farkas, D. K. Malick, A. D. Rabuck, K. Raghavachari, J. B. Foresman, J. V. Ortiz, Q. Cui, A. G. Baboul, S. Clifford, J. Cioslowski, B. B. Stefanov, G. Liu, A. Liashenko, P. Piskorz, I. Komaromi, R. L. Martin, D. J. Fox, T. Keith, M. A. Al-Laham, C. Y. Peng, A. Nanayakkara, M. Challacombe, P. M. W. Gill, B. Johnson, W. Chen, M. W. Wong, C. Gonzalez and J. A. Pople, *Gaussian 03 Revisions B.4, B.5, and C.1*, Gaussian, Inc., Pittsburgh, PA, 2003.
- 43 A. D. Becke, *J. Chem. Phys.*, 1993, **98**, 5648.
- 44 C. Lee, W. Yang and R. G. Parr, *Phys. Rev. B*, 1988, **37**, 785.
- 45 P. J. Stephens, F. J. Devlin, C. F. Chabalowski and M. J. Frisch, *J. Phys. Chem.*, 1994, **98**, 11623.
- 46 W. R. Wadt and P. J. Hay, *J. Chem. Phys.*, 1985, **82**, 284.
- 47 P. C. Hariharan and J. A. Pople, *Theor. Chim. Acta*, 1973, **28**, 213.
- 48 G. A. Petersson and M. A. Al-Laham, *J. Chem. Phys.*, 1991, **94**, 6081.
- 49 G. A. Petersson, A. Bennett, T. G. Tensfeldt, M. A. Al-Laham, W. A. Shirley and J. Mantzaris, *J. Chem. Phys.*, 1988, **89**, 2193.
- 50 *Apex2, Version 2 User Manual, M86-E01078*, Bruker Analytical X-ray Systems, Madison, WI, June 2006.
- 51 A. Altomare, G. Cascarano, G. Giacovazzo, A. Guagliardi, M. C. Burla, G. Polidori and M. Camalli, *J. Appl. Cryst.*, 1994, **27**, 435.
- 52 (a) P. W. Betteridge, J. R. Carruthers, R. I. Cooper, K. Prout and D. J. Watkin, *J. Appl. Crystallogr.*, 2003, **36**, 1487; (b) D. J. Watkin, C. K. Prout and L. J. Pearce, *CAMERON, Chemical Crystallography Laboratory*, Oxford, UK, 1996.
- 53 R. I. Cooper, A. L. Thompson and D. J. Watkin, *J. Appl. Crystallogr.*, 2010, **43**, 1100.